



FULL-LENGTH ARTICLE

Basic Research

Cytotoxic activity of anti-mucin 1 chimeric antigen receptor T cells expressing PD-1-CD28 switch receptor against cholangiocarcinoma cells

Kamonlapat Supimon^{1,2}, Thanich Sangsuwannukul^{1,2}, Jatuporn Sujitjoon^{1,2}, Thaweesak Chieochansin^{1,2}, Mutita Junking^{1,2,*}, Pa-thai Yenchitsomanus^{1,2,*}

¹ Siriraj Center of Research Excellence for Cancer Immunotherapy (SiCORE-CIT), Research Department, Faculty of Medicine Siriraj Hospital, Mahidol University, Bangkok, Thailand

² Division of Molecular Medicine, Research Department, Faculty of Medicine Siriraj Hospital, Mahidol University, Bangkok, Thailand

ARTICLE INFO

Article History:

Received 12 April 2022

Accepted 11 October 2022

Key Words:

chimeric antigen receptor T cells
 cholangiocarcinoma
 mucin 1
 programmed death-ligand 1
 switch receptor

ABSTRACT

Background aims: Cholangiocarcinoma (CCA) is a lethal bile-duct cancer that is difficult to treat by current standard procedures. This drawback has prompted us to develop adoptive T-cell therapy for CCA, which requires an appropriate target antigen for binding of chimeric antigen receptor (CAR) T cells. Mucin 1 (MUC1), an overexpressed protein in CCA cells, is a potential target antigen for the CAR T-cell development. However, MUC1 overexpression also is associated with the upregulation of programmed death-ligand 1 (PD-L1), an immune checkpoint protein that prohibits anti-tumor functions of T cells, probably causing poor overall survival of patients with CCA.

Methods: To overcome this problem, we developed anti-MUC1-CAR T cells containing PD-1-CD28 switch receptor (SR), namely α M.CAR/SR T cells, to target MUC1 and switch on the inhibitory signal of PD-1/PD-L1 interaction to activate CD28 signaling. Our lentiviral construct contains the sequences that encode anti-MUC1-single chain variable fragment, CD137 and CD3 ζ , linked with P2A, PD-1 and CD28.

Results: Initially, the upregulations of MUC1 and PD-L1 proteins were confirmed in CCA cell lines. α M.CAR and SR were co-expressed in $53.53 \pm 13.89\%$ of transduced T cells, mainly CD8 $^{+}$ T cells ($85.7 \pm 0.75\%$, $P < 0.0001$) with the effector memory phenotype ($59.22 \pm 16.31\%$, $P < 0.01$). α M.CAR/SR T cells produced high levels of intracellular tumor necrosis factor- α and interferon- γ in response to the activation by CCA cells expressing MUC1, including KKU-055 ($27.18 \pm 4.38\%$ and $27.33 \pm 5.55\%$, respectively, $P < 0.05$) and KKU-213A ($47.37 \pm 12.67\%$ and $54.55 \pm 8.66\%$, respectively, $P < 0.01$). Remarkably, the cytotoxic function of α M.CAR/SR T cells against KKU-213A cells expressing PD-L1 was significantly enhanced compared with the α M.CAR T cells ($70.69 \pm 14.38\%$ versus $47.15 \pm 8.413\%$, respectively; $P = 0.0301$), correlated with increased granzyme B production ($60.6 \pm 9.89\%$ versus $43.2 \pm 8.95\%$, respectively; $P = 0.0402$). Moreover, the significantly enhanced disruption of KKU-213A spheroids by α M.CAR/SR T cells ($P = 0.0027$), compared with α M.CAR T cells, was also observed.

Conclusion: Taken together, the cytotoxic function of α M.CAR/SR T cells was enhanced over the α M.CAR T cells, which are potential to be further tested for CCA treatment.

© 2022 International Society for Cell & Gene Therapy. Published by Elsevier Inc. All rights reserved.

Introduction

Cholangiocarcinoma (CCA) is a heterogenous biliary-tree cancer with a high mortality rate [1]. Surgery is the most effective treatment

for localized cancers; however, the recurrent rate after the surgery is as high as ~70–80% [2]. For the treatment of advanced CCA, chemotherapy, liver-directed therapies, targeted therapies and immunotherapies are not effective to cure the disease and also cause adverse side effects [3]. Recently, immunotherapies have emerged as alternative treatments for CCA [4]; however, the clinical data are limited. Moreover, immune escape mechanisms and the immunosuppressive tumor microenvironment of CCA are major challenges for the development of the immunotherapies against CCA [5]. Thus, more efficient therapeutic options for CCA are urgently needed.

* Correspondence: Asst. Prof. Mutita Junking, Mahidol University, Research Department, Siriraj Center of Research Excellence for Cancer Immunotherapy (SiCORE-CIT) and Division of Molecular Medicine, Faculty of Medicine Siriraj Hospital, Bangkok 10700, Thailand.

E-mail addresses: mjunking@gmail.com (M. Junking), ptyenchi@gmail.com, pathai.yen@mahidol.edu (P.-t. Yenchitsomanus).

Mucin 1 (MUC1) protein is reported to overexpress in most (50–87%) of the CCA tissue samples in the studies from several countries [6–8]. MUC1 overexpression was found to correlate with poor prognosis and low survival rate of patients with CCA [9]. MUC1 is a transmembrane protein that is expressed on the apical surface of epithelial cells [10]. Normally, the extracellular domain of MUC1 is heavily glycosylated at the variable number tandem repeat region, which provides mucous formation to protect the cells from pathogen access, maintenance of cell lubrication and protection of cell desiccation [10]. In addition, the intracellular domain of MUC1 can be phosphorylated and plays role in signal transduction [10,11]. In several cancers, tumor-associated MUC1 with a low level of glycosylation is overexpressed and miss-located on the cell membrane. These aberrant phenotypes induce cancer progression by promoting apoptotic resistance, angiogenesis, cell proliferation, invasion and metastasis [10]. Importantly, MUC1 upregulation mediated the increased programmed death-ligand 1 (PD-L1) expression, which could subsequently inhibit T cell functions in breast and non-small cell lung cancers [12–14]. However, the correlation between MUC1 overexpression and PD-L1 upregulation in CCA has not been documented previously.

PD-L1, an immune checkpoint ligand, is a transmembrane protein that is constitutively expressed on the membrane of antigen-presenting cells (APCs), including macrophages, B cells and dendritic cells. It is also observed on endothelial, islet and pancreatic cells [15]. PD-L1 expression plays a role in controlling immune responses and preventing autoimmune damages by inhibition of T-cell proliferation, survival and cytokine production [15]. PD-L1 functions by engagement with its receptor, programmed cell death protein-1 (PD-1), which is inducible to express on the activated immune cells such as T, B and natural killer (NK) cells [15]. PD-1/PD-L1 interaction initiates the recruitment of Src homology region 2 domain-containing phosphatase 2, which dephosphorylates important molecules for T-cell activation, such as leukocyte-specific tyrosine kinase, phospholipase C gamma 1 and phosphoinositide-3-kinase/Akt [16]. Importantly, PD-L1 expression is an immune escape mechanism of cancer cells [17] that is observed in approximately 70% (32/46) of tissues of Thai patients with CCA [18] and 71% (125/175) of tissues of Korean patients with CCA [19] with advanced disease. Thus, PD-L1 expression in CCA tissues is a problem that needs to be overcome in the development of therapeutic approaches.

Adoptive T-cell therapy using chimeric antigen receptor (CAR) T cells is a promising treatment for CCA. CAR T cells are genetically engineered T cells that express receptors recognizing surface antigens on cancer cells and induce cancer cell apoptosis without antigen presentation on major histocompatibility complex molecules [20]. The second-generation CAR T cells targeting CD19 have been approved by the US Food and Drug Administration for the treatment of relapsed or refractory B-cell acute lymphoblastic leukemia [21]. However, the anti-tumor efficacies of CAR T-cell therapy in patients with solid cancers are limited because of their complicated tumor microenvironment [20]. Anti-MUC1-CAR T cells have been studied in breast, head and neck, non-small cell lung, pancreatic and hematological cancers [22–26]. Our group has recently reported the effectiveness of anti-MUC1-CAR T cells against a CCA model [27]. These CAR T cells showed impressive anti-tumor functions by promoting cancer cell lysis and increasing anti-tumor cytokine production. Some of the anti-MUC1-CAR T cells were further studied in clinical trials; however, none of them has been approved for clinical use [28]. To improve the efficiency of CAR T-cell therapy and overcome the immune escape mechanism of cancers, modified CAR T cells were generated with additional of receptor molecules, for example, inverted cytokine receptor (interleukin [IL]-4R/IL-7R) [24], CAR T cells secreting IL-12 [29] and switch receptor (SR) molecules, PD-1-CD28 [30–32]. Here, we aimed to combine anti-MUC1 CAR T cells and the latter strategy as the upregulation of MUC1 in cancer cells could

mediate the expression of PD-L1 [12–14]. Thus, by simultaneously targeting MUC1- and PD-L1-expressing cancer cells using anti-MUC1-CAR and SR molecules, PD-1-CD28 (PD-1 extracellular domain linked with CD28 intracellular domain) would provide better anti-tumor activity and overcome immune escape in solid tumors. In the present study, we created anti-MUC1-CAR (α M.CAR) T cells containing SR molecules (PD-1-CD28), namely α M.CAR/SR T cells, to target MUC1 and PD-L1 proteins on CCA cells. The cytotoxic function of the α M.CAR/SR T cells was pre-clinically evaluated on CCA cells overexpressing both MUC1 and PD-L1 proteins

Materials and Methods

Cell lines and culture condition

The immortal cholangiocytes (MMNK-1), CCA cells (KKU-055 and KKU-213A), HEK293T and Lenti-X 293T cells were maintained in Gibco Dulbecco's Modified Eagle Medium, and KKU-100 cells were cultured in Gibco Dulbecco's Modified Eagle Medium/Nutrient Mixture F-12, supplemented with 10% heat-inactivated fetal bovine serum (FBS) and 100 μ g/mL streptomycin and penicillin. The characteristics of cholangiocytes and CCA cell lines are provided in supplementary Table 2. Peripheral blood mononuclear cells (PBMCs) isolated from whole-blood samples of healthy donors were maintained in Roswell Park Memorial Institute Medium (RPMI-1640) containing 5% heat-inactivated human AB serum and 100 μ g/mL streptomycin and penicillin (completed RPMI-1640). Phytohemagglutinin L (PHA-L)-activated lymphocytes were cultured in cytoRPMI-1640 containing recombinant human (rh) cytokines including 0.02 μ g/mL IL-2, 0.01 μ g/mL IL-7 and 0.04 μ g/mL IL-15 (ImmunoTools, Friesoythe, Germany).

Generation of CCA cells overexpressing MUC1

HEK293T cells were transfected with SFG plasmid containing *MUC1* cDNA, kindly provided by Dr. John Maher, King's College London [22], and packaging plasmids including VSV-G and pGP1 by calcium phosphate-based method and concentrated by centrifugation at 20,000 \times g for 3 hours (h) at 4°C. The CCA parental KKU-055, KKU-100 and KKU-213A cells were transduced using retrovirus and centrifugation at 1,200 \times g for 90 minutes (min) at 32°C.

Generation of α M.CAR and α M.CAR/SR lentiviral constructs

A lentiviral (pCDH) vector containing *anti-MUC1-CAR* (α M.CAR) [27] and SR (PD-1-CD28) were constructed. The SR (PD-1-CD28) sequence was synthesized by Integrated DNA Technologies (Coralville, IA, USA), amplified and subcloned into α M.CAR containing lentiviral vector (supplementary Table 1). The *anti-MUC1-CAR* (α M.CAR) was composed of (i) a single-chain variable fragment of HMFG2 monoclonal antibody against MUC1 linked with IgD and IgG1Fc hinge domains, and (ii) CAR2 cassette sequence including transmembrane domain of CD8 and intracellular domain of CD137 and CD3 ζ . Positive clones containing either α M.CAR or α M.CAR/SR sequence were screened by colony polymerase chain reaction and confirmed by Sanger DNA sequencing (supplementary Figs. 2 and 3).

PBMC isolation and cell activation

Whole-blood samples were collected from healthy donors following the experimental protocol and informed consent approved by the Siriraj Institutional Review Board (number Si 101/2020). The whole blood samples mixed with Corning lymphocyte separation medium (Corning Inc., Corning, NY, USA). The PBMCs were plated for 3–6 h and adherence monocytes were removed to obtain lymphocytes,

which were then activated with 5 µg/mL PHA-L (Roche, Basel, Switzerland) for 3 days.

Transfection and viral packaging

The anti-MUC1-CAR (α M.CAR) and anti-MUC1-CAR/SR (α M.CAR/SR) constructs were transfected into HEK293T cells by using lipofectamine 2000 (Thermo Fisher Scientific, Waltham, MA, USA). After 48 h, the transfected cells were collected and the expressions of α M.CAR and PD-1-CD28 proteins were examined by immunoblotting assay and flow cytometry.

Lentiviral particles containing α M.CAR or α M.CAR/SR were produced by transfection of α M.CAR or α M.CAR/SR construct into Lenti-X 293T cells (Takara Bio Inc., Shiga, Japan) using a calcium phosphate-based method following the standard protocol, together with the packaging plasmids pMD2.G and psPAX2. At 48 and 72 h, lentiviral particles in the supernatant were collected and concentrated by centrifugation at 20,000×g for 3 h at 4°C.

Production of α M.CAR T and α M.CAR/SR T cells

Healthy donor T cells were double transduced in a 24-well plate coated with 10 µg/mL Retronectin (Takara Bio Inc., Shiga, Japan) using lentiviral particles of the α M.CAR or α M.CAR/SR and centrifugation at 1,200×g for 90 min at 32°C in the presence of 10 µg/mL of protamine sulfate (Mochida Pharmaceutical Co., Ltd., Tokyo, Japan). Cells were maintained in cytoRPMI-1640 medium. Similar procedures without lentiviral particles were performed to obtain untransduced (UTD) cell control. The α M.CAR and PD-1-CD28 molecules expressed on the membrane of transduced cells were detected by flow cytometry.

Immunoblotting assay

The α M.CAR- and α M.CAR/SR-transfected HEK293T cells were harvested after 48 h of transfection. Cell lysates were then separated on sodium dodecyl sulfate-polyacrylamide gel electrophoresis, transferred onto a nitrocellulose membrane and blocked with 5% skim milk for 1 h. The blotted membrane was probed with anti-CD3ζ antibody (Santa Cruz Biotechnology, Santa Cruz, CA, USA). The cell lysates prepared from lymphocytes were used as a positive control. The protein intensity was determined by using ImageJ (National Institutes of Health, Bethesda, MD, USA) and normalized with glyceraldehyde 3-phosphate dehydrogenase.

Cell proliferation

The MMNK-1 and KKU-213A cells were plated in a 24-well plate and co-cultured with either UTD T, α M.CAR T or α M.CAR/SR CAR T cells at effector-to-target ratio (E:T) of 1:10. The effector T cells were then collected on day 3 and day 7 and counted by using Countess II FL Automated Cell Counter (Thermo Fisher Scientific). The total cell counts were plotted as a bar graph of fold-change normalized by the numbers of CAR T cells seeded on the first day of the co-culturing (day 0).

Flow cytometry

The expression of MUC1 and PD-L1 was examined by flow cytometry under non-permeabilized conditions. The cells were stained with 1:50 dilution of anti-MUC1 antibody (EP1024Y; Abcam, Cambridge, UK) and with 1:100 dilution of anti-PD-L1-PE antibody (BioLegend, San Diego, CA, USA) in 2% FBS/1× phosphate-buffered saline (PBS) for 2 h. The Alexa Fluor 488 dye-conjugated secondary antibody (Invitrogen, Carlsbad, CA, USA) at 1:500 dilution was added and incubated for 1 h.

The anti-MUC1-CAR (α M.CAR) and SR (PD-1-CD28) proteins were detected on the surface of transfected HEK293T or transduced T cells by staining with anti-human Fcγ-APC (Jackson ImmunoResearch Laboratories, Inc., West Grove, PA, USA) and anti-PD-1-PE antibodies (Invitrogen). Briefly, cells were stained with anti-human Fcγ-APC antibody (1:1,000) for 45 min. After washing, the anti-PD-1-PE antibody (1:100) was added and incubated for 45 min.

For cellular phenotypes including T-cell subsets, exhaustion and activation markers, anti-CD3-FITC, CD4-APC, CD8-APC, CD19-APC, CD16-APC, CD62L-APC and CD69-APC (ImmunoTools GmbH, Friesoythe, Germany), anti-CD45RA-PE-cyanine7 (Invitrogen), anti-CD25-PerCP-cyanine5.5 (eBioscience, San Diego, CA, USA) and anti-CD56-PE, LAG-3-PE and TIM-3-PE (BioLegend) were used. Cells were stained with the 1:100 dilution of antibodies in 2% FBS/1×PBS for 45 min before analyses. All data were acquired on BD FACSVerser (BD Biosciences, Franklin Lakes, NJ, USA) and analyzed with FlowJo software version 10.

Intracellular cytokine and granzyme B detection

The UTD T, α M.CAR T and α M.CAR/SR T cells were co-cultured with or without target cells (MMNK-1, KKU-055 and KKU-213A), at E:T ratio of 5:1 for 1 h. Then, brefeldin A was added and further incubated at 37°C in a humidified 50 mL/L CO₂ atmosphere for 5 h. The UTD T, α M.CAR T and α M.CAR/SR T cells were collected and stained with anti-CD3-FITC and CD8-APC antibodies for 45 min. After fixation with 1% formaldehyde for 10 min, the cells were permeabilized and stained with anti-tumor necrosis factor (TNF)-α-phycoerythrin (PE), interferon (IFN)-γ-PE or granzyme B-FITC antibody (ImmunoTools GmbH) in 0.5% saponin for 45 min. Intracellular TNF-α, IFN-γ and granzyme B production was detected by a flow cytometer.

Cytokine bead array (CBA)

The UTD T, α M.CAR T or α M.CAR/SR T cells were co-cultured with KKU-213A cells at an E:T ratio of 5:1 in AIM-V medium containing 5% heat-inactivated human AB serum without the addition of cytokines. After 24 h of co-culture, the cells were separated by centrifugation and culture supernatants were collected. The levels of multiple cytokines were measured by CBA using the LEGENDplex Human CD8/NK Panel (BioLegend) by following the manufacturer's protocol. Cytokine levels were normalized with the culture supernatant of target cells alone and plotted as bar graphs of fold-change compared with those of the UTD T cells.

Killing activity and fluorescence detection

The MMNK-1, KKU-055 and KKU-213A cells were genetically engineered to stably express Wasabi (green fluorescence) and luciferase proteins. The target cells were cultured in a 96-well plate for 24 h. The UTD T, α M.CAR T and α M.CAR/SR T cells were added to the plate at E:T ratios of 1:1, 2.5:1 and 5:1 and further incubated for 24 h. The remaining target cells expressing Wasabi green fluorescence were detected by a fluorescence microscope (Nikon, Tokyo, Japan).

Luciferase assay

The UTD T, α M.CAR T and α M.CAR/SR T cells were co-cultured with the target (MMNK-1, KKU-055 and KKU-213A) cells expressing luciferase enzyme for 18 h. The UTD T, α M.CAR T and α M.CAR/SR T cells were then removed and the remaining target cells were washed once with 1×PBS. Luciferase activity of the remaining target cells was measured by using Pierce Firefly Luciferase Glow Assay Kit (Thermo Fisher Scientific) following a manufacturer's protocol and examined by a luminometer. The percentage of specific killings was calculated by the following formula:

$$\% \text{ specific killing} = 100 - \left(\frac{\text{Luciferase activity from well with effector and target cells}}{\text{Luciferase activity from well with only target cells}} \right) \times 100$$

Long-term co-culture assay

To examine tumor cell lysis in long-term co-culture assay, either UTD T, α M.CAR T or α M.CAR/SR T cells were added to KKU-213A cells, at an E:T ratio of 5:1 for 7 days. On days 1 and 7 after the co-culture, viable target cells were fixed and stained with 0.1% crystal violet (Sigma-Aldrich, St Louis, MO, USA) for 30 min. Then, the plates were washed thrice with water and dried overnight. The crystal violet dye was dissolved in 1% sodium dodecyl sulfate and subjected for reading out at optical density (O.D.) 570 nm by Synergy HTX Multi-Mode Microplate Reader (BioTek, Winooski, VT, USA). To examine expressions of exhaustion markers, the CAR T cells were co-cultured with KKU-213A cells at an E:T ratio of 2:1 for 7 days. Then, the effector T cells were harvested, stained with CD3-PerCP, CD8-FITC, LAG-3-PE and TIM-3-PE antibodies and then detected by flow cytometry.

KKU-213A spheroid killing assay

To study the cytotoxic function of the α M.CAR T and α M.CAR/SR T cells in a three-dimensional (3D) spheroid model, the Wasabi and luciferase-expressing KKU-213A cells (2×10^3 cells) were mixed on-ice with the Corning Matrigel Basement Membrane Matrix according to manufacturer's protocol and plated into Corning Ultra-Low Attachment Surface Products (Corning Inc.). After 48 h, tumor spheroids were separately prepared into four groups, (i) no treatment, (ii) cultured with UTD T cells, (iii) cultured with α M.CAR T and (iv) cultured with α M.CAR/SR T, by using an E:T ratio of 10:1. The KKU-213A spheroid structure were monitored at days 0, 1, 3 and 5 after the co-

culturing by using a fluorescence microscope (Nikon, Tokyo, Japan) and setting the objective lens at $10\times$ magnification. The corrected total cell fluorescence (CTCF) of KKU-213A spheroids was analyzed by ImageJ software [33]. The CTCFs of the UTD T, α M.CAR T cells and α M.CAR/SR T cells were normalized with the CTCF of the no-treatment group in the individual experiments each day. CTCF was calculated by the following formula:

$$\begin{aligned} \text{CTCF} &= \text{Integrated density} \\ &\quad - (\text{Area of selected cell} \times \text{Mean fluorescence of background readings}) \end{aligned}$$

Statistical analysis

The datasets were collected from at least three independent experiments. Statistical analysis was performed in GraphPad Prism version 7, GraphPad Software (San Diego, CA, USA; www.graphpad.com). Significant difference of the datasets was analyzed by the Student *t*-test (the asterisks indicate significant difference; **P* < 0.05, ***P* < 0.01, ****P* < 0.001, and *****P* < 0.0001). The graphs of mean \pm standard deviation obtained from at least three independent experiments were plotted.

Results

MUC1 overexpression mediates PD-L1 upregulation in CCA cells

PD-L1 overexpression in cancer cells is a major challenge of CAR T-cell therapy against solid tumors because it was able to impair anti-tumor functions of CAR T cells [34]. We then first examined the endogenous PD-L1 expression on parental CCA cell surfaces. Low PD-L1 expression was found in KKU-055 ($8.37 \pm 2.65\%$), moderate in KKU-100 ($47.96 \pm 1.32\%$) and high in KKU-213A ($97.39 \pm 0.56\%$) cells

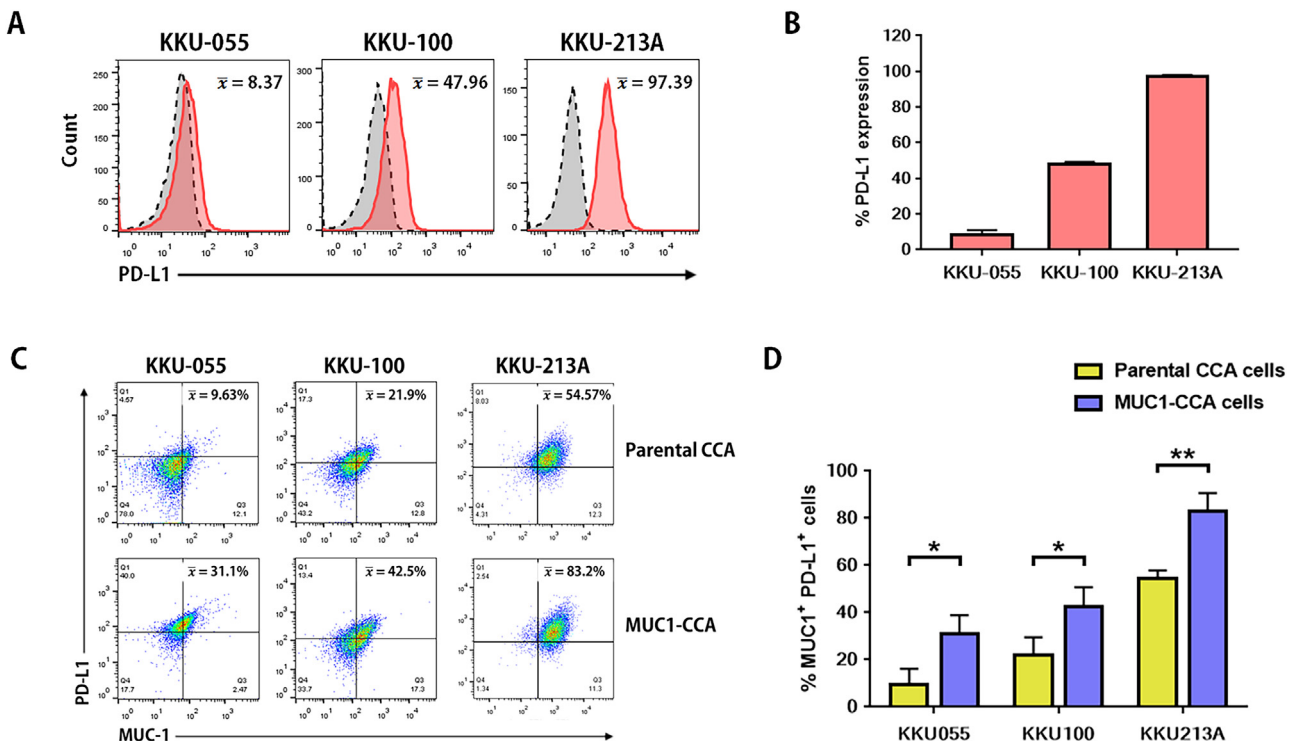


Fig. 1. PD-L1 expression in parental CCA cells and CCA cells overexpressing MUC1 detected by flow cytometry. (A) Endogenous PD-L1 expression on the surface of CCA cell lines. Gray peaks represent the fluorescent intensity of isotype control and red peaks are PD-L1-stained cells. (B) Percentages of PD-L1 expression were quantitated from three independent experiments (mean \pm standard deviation). (C) MUC1 and PD-L1 co-expression in parental CCA cells and CCA cells overexpressing MUC1 (MUC1-CCA). The data from three independent experiments were summarized as a bar graph (mean \pm standard deviation). (D) The yellow and blue bars are UTD and MUC1-transduced CCA cells, respectively. All datasets were analyzed by the Student *t*-test (asterisks indicate statistically significant differences: **P* < 0.05 and ***P* < 0.01). (Color version of figure is available online.)

(Fig. 1A,B). MUC1 expression in CCA cells was shown in our previous report [27]. Here, we overexpressed MUC1 in CCA cells by using retroviruses carrying *MUC1* cDNA and investigated whether PD-L1 is altered. Interestingly, significantly increased PD-L1 expressions were found in the CCA cells overexpressing MUC1 (Fig. 1C, supplementary Fig. 1). The MUC1-overexpressed CCA cells showed significant greater levels of MUC1 and PD-L1 co-expressed population, KKU-055 (from $9.633 \pm 6.47\%$ to $31.1 \pm 7.74\%$, $P = 0.0212$), KKU-100 (from $21.9 \pm 7.63\%$ to $42.5 \pm 8.29\%$, $P = 0.034$) and KKU-213A cells (from $54.57 \pm 3.32\%$ to $83.2 \pm 7.43\%$, $P = 0.0037$), compared with the parental cells (Fig. 1D). Our results demonstrated that the greater MUC1 expression could affect levels of PD-L1 expression on the CCA cell surface and could be targetable by dual MUC1 and PD-L1 CAR T-cell strategy.

Anti-MUC1-CAR with SR lentiviral vector was successfully constructed and their proteins were expressed in mammalian HEK293T cells

The schematic diagrams of lentiviral constructs containing anti-MUC1-CAR (α M.CAR) or anti-MUC1-CAR linked with PD-1-CD28 SR (α M.CAR/SR) are shown in Fig. 2A. We initially examined whether our CAR-containing lentiviral vectors were able to express α M.CAR and PD-1-CD28 proteins in mammalian HEK293T cells (Fig. 2B–E) and found that the α M.CAR molecule containing CD3 ζ was detected

in both α M.CAR- and α M.CAR/SR-transfected cells (Fig. 2B, supplementary Fig. 4). Surface expression of α M.CAR and α M.CAR/SR also was confirmed ($93.53 \pm 10.85\%$ and $93.33 \pm 10.35\%$, respectively), compared with untransfected cells. The PD-1-CD28 SR was significantly found on the surface of α M.CAR/SR-transfected cells ($97.93 \pm 1.19\%$), compared with the α M.CAR-transfected cells and untransfected cells (all $P < 0.0001$) (Fig. 2C–E). The co-expression of the α M.CAR and PD-1-CD28 molecules was found only in the α M.CAR/SR-transfected cells at the level of $91.23 \pm 8.39\%$ (Fig. 2D). Therefore, we successfully created the lentiviral vectors expressing α M.CAR and α M.CAR/SR which could be expressed in the mammalian cell system.

Successful generation of α M.CAR T cells and α M.CAR/SR T cells

α M.CAR T cells and α M.CAR/SR T cells were then generated by lentiviral transduction. The expressions of α M.CAR and PD-1-CD28 molecules on the surface of CAR T cells were evaluated. The addition of SR did not affect the transduction efficacy of α M.CAR constructs, as there was no significant difference transduction efficacy between the α M.CAR T cells and α M.CAR/SR T cells. Significantly greater transduction efficacy of α M.CAR compared with UTD T cells was found ($P < 0.0001$), $53.35 \pm 11.93\%$ of α M.CAR T cells and $57.85 \pm 13.44\%$ of α M.CAR/SR T cells. In addition, significantly greater expression of PD-1-

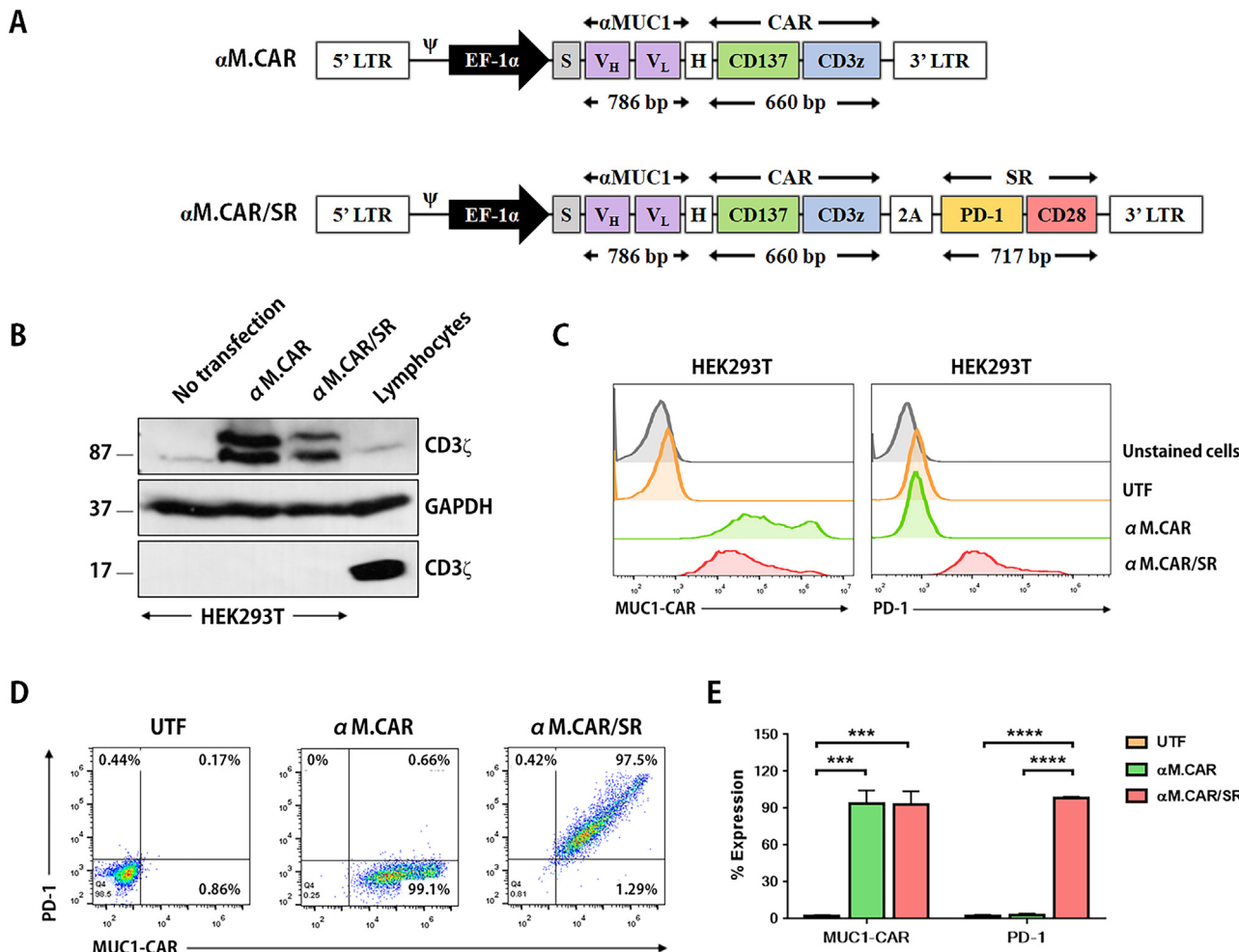


Fig. 2. Schematic diagrams of α M.CAR and α M.CAR/SR lentiviral constructs and evaluation of α M.CAR and PD-1-CD28 protein expression in mammalian cells. (A) Schematic diagrams of α M.CAR and α M.CAR/SR lentiviral constructs. S is a signal sequence, H represents the hinge region (spacer), and 2A represents the self-cleaving peptide. (B) Immunoblotting of CD3 ζ protein collected from α M.CAR and α M.CAR/SR transfected HEK293T cells. Glyceraldehyde 3-phosphate dehydrogenase was used as a loading control. (C) Cell surface expression of α M.CAR and PD-1-CD28 proteins on transfected HEK293T cells were detected by flow cytometry. (D) Gating of the membranous α M.CAR and PD-1-CD28 expression compared with untransfected (UTF) cells. (E) Percentages of α M.CAR and PD-1-CD28 expression on the cell surface were analyzed from three independent experiments (mean \pm standard deviation); color codes: orange, green, and pink are the protein expression on UTF, α M.CAR, and α M.CAR/SR transfected cells, respectively. The statistical datasets were analyzed by Student *t*-test (**P < 0.001, and ****P < 0.0001). (Color version of figure is available online.)

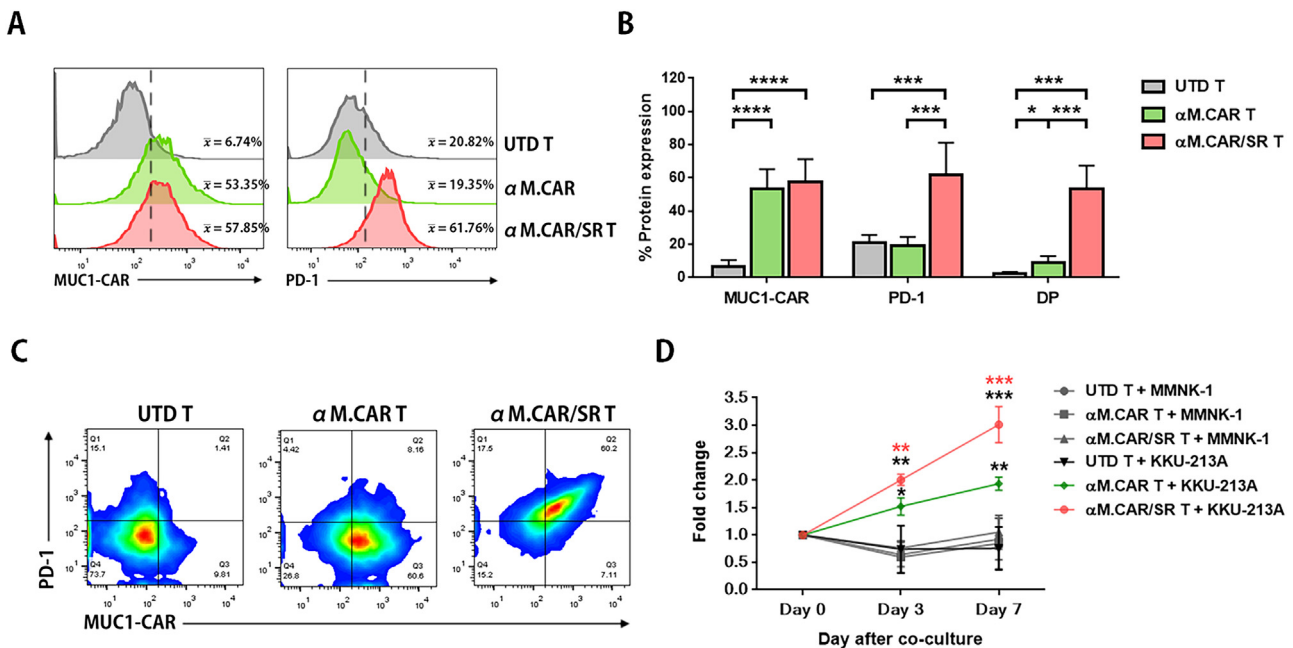


Fig. 3. Production and proliferation analysis of αM.CAR T and αM.CAR/SR T cells. (A) αM.CAR and PD-1-CD28 expression on the cell surface of UTD T cells (gray), αM.CAR T cells (green) and αM.CAR/SR T cells (red). (B) Percentages of αM.CAR and PD-1-CD28 expression were analyzed from six independent experiments (mean \pm standard deviation). Double-positive (DP) are the cells that expressed both αM.CAR and PD-1-CD28 molecules on their cell surface. (C) Gating of the αM.CAR and PD-1-CD28 analyzed on the UTD T, αM.CAR T and αM.CAR/SR T cells. (D) Proliferation analysis UTD T, αM.CAR T and αM.CAR/SR T cells co-cultured with MMNK-1 or KKU-213A cells. The black asterisks are the statistical comparison of cell proliferation between the CAR T and UTD T cells. The red asterisks are the comparison between the αM.CAR T and αM.CAR/SR T cells. The datasets were analyzed from three independent experiments (mean \pm standard deviation) and analyzed by the Student *t*-test (asterisks indicate statistically significant differences: * P < 0.05, ** P < 0.01, *** P < 0.001, and **** P < 0.0001). (Color version of figure is available online.)

CD-28 SR was found only on the αM.CAR/SR T cells ($61.76 \pm 19.47\%$, $P \leq 0.0005$), whereas the endogenous PD-1 on the αM.CAR T cells and UTD T cells was similar ($19.35 \pm 5.14\%$ and $20.82 \pm 4.89\%$, respectively). The co-expression of the αM.CAR and PD-1 molecules was detected on the surface of αM.CAR/SR T cells ($53.53 \pm 13.89\%$, $P \leq 0.0008$), compared with that on the αM.CAR T cells ($8.85 \pm 4.08\%$) and the UTD T cells ($2.32 \pm 1.01\%$) (Fig. 3A–C).

Proliferation of αM.CAR T cells and αM.CAR/SR T cells in response to exposure to CCA cells expressing MUC1 and PD-L1

To examine T-cell proliferation after tumor exposure, αM.CAR T cells and αM.CAR/SR T cells were co-cultured with either low MUC1-expressing immortal cholangiocytes MMNK-1 ($4.027 \pm 0.994\%$) or high MUC1- and PD-L1-expressing parental KKU-213A cells ($58.81 \pm 12.59\%$) (supplementary Fig. 1A, Fig. 1A). After exposure to MMNK-1 cells, the numbers of the UTD T cells, αM.CAR T cells and αM.CAR/SR T cells were not significantly different (Fig. 3D). However, significant T-cell proliferation was found after the αM.CAR T cells and αM.CAR/SR T cells were exposed to the KKU-213A compared with UTD T cells ($P = 0.0144$ and 0.0012 at day 3, and $P = 0.0012$ and 0.0001 at day 7, respectively) (Fig. 3D). Furthermore, enhanced T-cell proliferation was found in the αM.CAR/SR T cells, which was significantly greater than that of αM.CAR T cells on day 3 ($P = 0.0022$) and day 7 ($P = 0.0008$) (Fig. 3D). Thus, our results showed MUC1-specific T-cell proliferation in the αM.CAR T cells and αM.CAR/SR T cells in response to exposure of CCA cells expressing MUC1, and this could be promoted by the addition of SR as shown in the αM.CAR/SR T cells.

αM.CAR/SR T cells contained CD8⁺ T cells, effector memory T cells and low exhaustion markers

To study T-cell subsets, unactivated PBMCs, activated lymphocytes, αM.CAR T cells and αM.CAR/SR T cells were stained using

phenotypic, exhaustion, and activation markers (Fig. 4). The gating strategies of cell phenotypes are shown in supplementary Fig. 5. The cytotoxic T cells were significantly increased in activated lymphocytes ($81.57 \pm 4.25\%$, $P = 0.0001$), αM.CAR T cells ($86.23 \pm 2.69\%$, $P < 0.0001$) and αM.CAR/SR T cells ($85.7 \pm 0.76\%$, $P < 0.0001$) compared with unactivated PBMCs ($40.6 \pm 1.93\%$). In contrast, αM.CAR T cells and αM.CAR/SR T cells showed significantly reduced percentages of helper T cells (from $37.93 \pm 2.77\%$ to $12.52 \pm 2.48\%$ and $13.57 \pm 1.95\%$, $P < 0.001$), B cells (from $6.373 \pm 2.49\%$ to $0.09 \pm 0.06\%$ and $0.05 \pm 0.05\%$, $P < 0.05$) and NK cells (from $9.13 \pm 0.91\%$ to $2.13 \pm 0.5\%$ and $1.53 \pm 0.63\%$, $P < 0.001$). In addition, the NKT cells were reduced in αM.CAR T cells and αM.CAR/SR T cells ($2.43 \pm 1.49\%$, $P = 0.066$, and $2.22 \pm 0.30\%$, $P = 0.0294$), compared with that of the unactivated PBMCs ($5.98 \pm 1.94\%$) (Fig. 4A,B), whereas there was no significant difference among αM.CAR and αM.CAR/SR T cells.

After activation and lentiviral transduction, increased LAG-3 and TIM-3 expressions were found in αM.CAR T cells ($P < 0.001$) and αM.CAR/SR T cells ($P < 0.005$) compared with unactivated PBMCs. However, significantly lower levels of exhaustion markers were found in the αM.CAR/SR T cells compared with αM.CAR T cells (LAG-3, $P = 0.025$, and TIM-3, $P = 0.0196$) (Fig. 4C,D). Also, significantly increased expression of CD25 and CD69 activation markers was found in αM.CAR ($P = 0.0003$ and $P = 0.0156$, respectively) and αM.CAR/SR T cells ($P = 0.0007$ and $P = 0.0053$, respectively), compared with that of the unactivated PBMCs (Fig. 4E).

T-cell subsets comprising naïve T cells (CD3⁺, CD45RA⁺, CD62L⁺), central memory T cells (T_{CM}; CD3⁺, CD45RA⁻, CD62L⁺), effector memory T cells (T_{EM}; CD3⁺, CD45RA⁻, CD62L⁻) and terminal effector T cells (T_{TE}; CD3⁺, CD45RA⁺, CD62L⁻) were evaluated (Fig. 4F, supplementary Fig. 5D). Compared with the unactivated PBMCs, naïve T cells were significantly reduced in the αM.CAR T cells and αM.CAR/SR T cells (from $51.04 \pm 14.6\%$ to $10.22 \pm 9.17\%$ and to $8.33 \pm 6.12\%$, both $P < 0.001$). The majorities of the αM.CAR T cells and αM.CAR/SR T cells were effector memory phenotype (increased from $21.04 \pm 10.11\%$ to $55.42 \pm 19.46\%$ and to $59.22 \pm 16.31\%$, respectively, both P

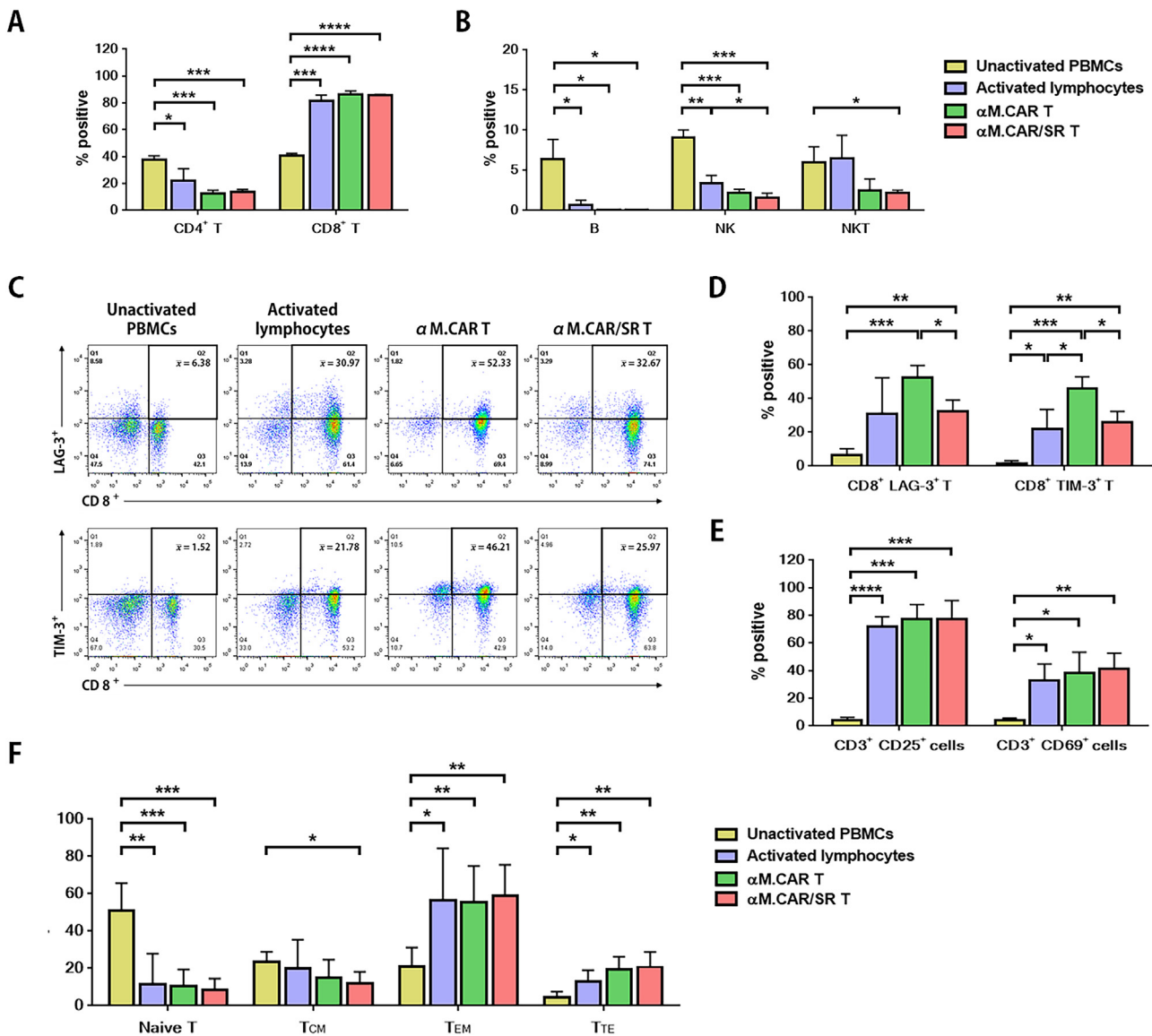


Fig. 4. Phenotypic verification of αM.CAR T and αM.CAR/SR T cells was analyzed by flow cytometry. The color codes are as follows: yellow denotes unactivated PBMCs, purple is activated lymphocytes, green is αM.CAR T, and red is αM.CAR/SR T cells. Percentages of (A) helper (CD4⁺) T cells, and cytotoxic (CD8⁺) T cells, (B) B (CD19⁺) cells, NK (CD15⁺ CD56⁺) cells, and NKT cells. (C) Gating of CD8⁺ LAG-3⁺ and CD8⁺ TIM-3⁺ cells from CD3⁺ population. Percentages of the cells expressing (D) exhaustion and (E) activation markers. The percentages of cell phenotypes, exhaustion and activation markers were analyzed from 3 independent experiments (mean ± standard deviation). (F) Percentage of the T-cell subsets: naïve T, central memory T (T_{CM}), effector memory T (T_{EM}) and terminal effector T (T_{TE}) cells. The datasets were summarized from 5 independent experiments (mean ± standard deviation). The statistical analysis was performed by the Student t-test (*P < 0.05, **P < 0.01, ***P < 0.001, and ****P < 0.0001). (Color version of figure is available online.)

< 0.01). Terminal effector cells also were increased in the αM.CAR T cells and αM.CAR/SR T cells (from 4.44 ± 3.09% to 19.42 ± 6.89% and to 20.7 ± 8.11%, both P < 0.01).

αM.CAR/SR T cells increased production of cytokines after exposure to CCA cells expressing MUC1 and PD-L1

To investigate anti-tumor functions of the αM.CAR T and αM.CAR/SR T cells against CCA cells expressing MUC1 and PD-L1, CAR T cells were co-cultured with MMNK-1, KKU-055 and KKU-213A, and intracellular TNF-α and IFN-γ productions were measured by flow cytometry. After exposure to KKU-055 cells, TNF-α was significantly elevated in αM.CAR T (29.32 ± 1.78%, P = 0.0011) and αM.CAR/SR T cells (27.18 ± 4.38%, P = 0.006), when compared with that of the UTD T cells (9.68 ± 3.67%). Similarly, when co-cultured with KKU-213A cells, αM.CAR T and αM.CAR/SR T cells upregulated TNF-α production (from 9.2 ± 4.65% to 23.87 ± 1.85% and to 47.37 ± 12.67%, respectively; both P < 0.01) (Fig. 5A,C). IFN-γ production of αM.CAR T

(26.13 ± 2.49%) and αM.CAR/SR T cells (27.33 ± 5.55%) also was significantly induced after co-culturing with KKU-055 cells (P = 0.0339 and P = 0.0456, respectively), compared with UTD T cells (12.58 ± 6.97%). The co-culturing of the αM.CAR T and αM.CAR/SR T cells with KKU-213A cells showed greater IFN-γ production (from 22.08 ± 6.11% to 37.9 ± 10.1%, P = 0.0364, and to 54.55 ± 8.67%, P = 0.0009, respectively) (Fig. 5B,D). Interestingly, αM.CAR/SR T cells showed enhanced TNF-α and IFN-γ cytokine production in response to PD-L1-expressing KKU-213A cells when compared with that of αM.CAR T cells without SR molecules (P = 0.0335 and P = 0.0464, respectively). In contrast, the αM.CAR T and αM.CAR/SR T cells demonstrated no significant difference in TNF-α (7.14 ± 6.52%, 5.83 ± 4.74%, and 7.83 ± 6.52%, respectively) and IFN-γ production (12.76 ± 5.65%, 10.83 ± 4.21%, and 13.61 ± 6.55%, respectively) in response to low MUC1-expressing MMNK-1 cells compared with that of UTD T cells. Therefore, our results demonstrated MUC1-specific responses of CAR T cells and the addition of SR molecules could promote TNF-α and IFN-γ production of αM.CAR/SR T cells.

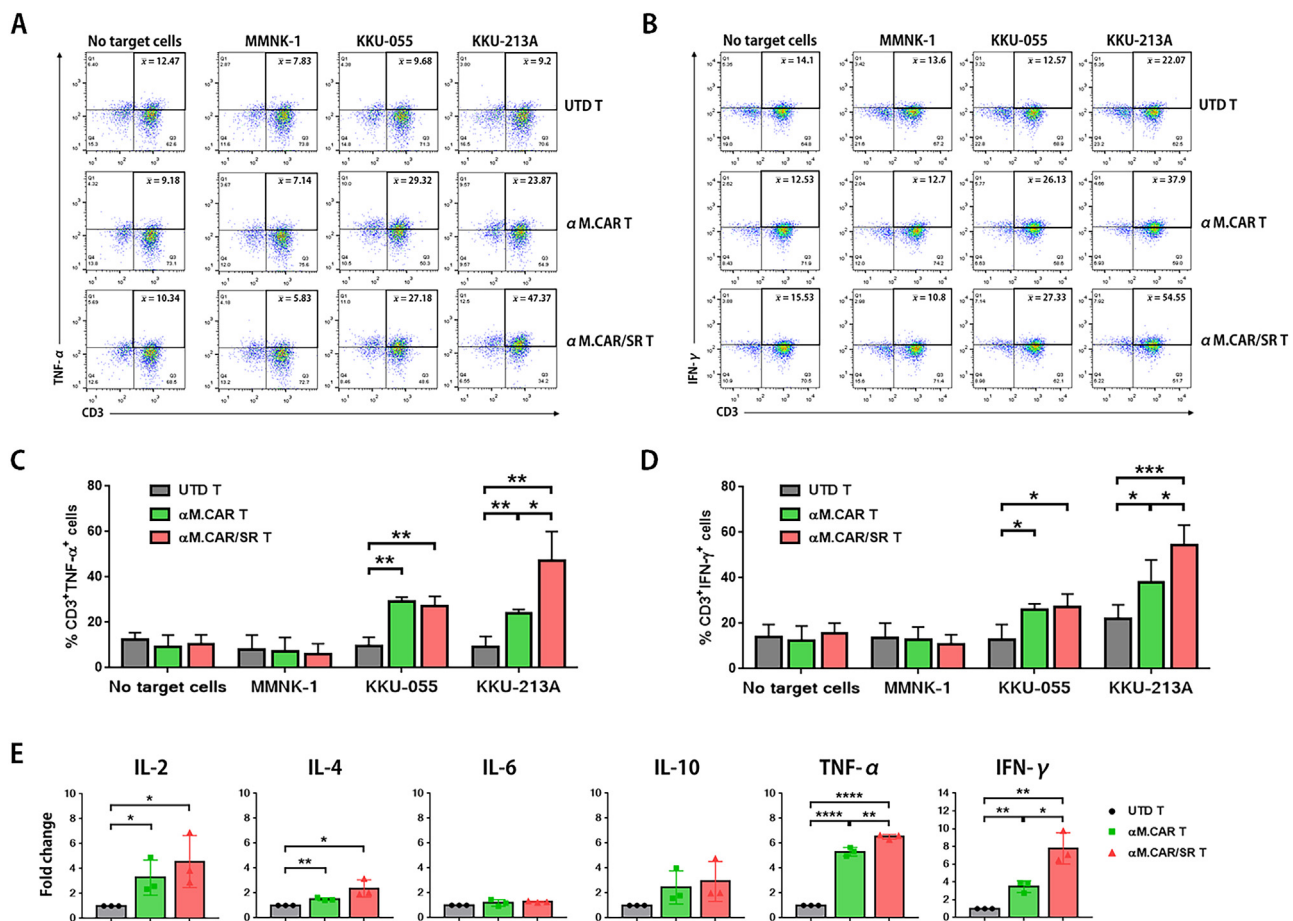


Fig. 5. Intracellular TNF- α and IFN- γ cytokine production of α M.CAR T and α M.CAR/SR T cells in response to the exposure to MMNK-1, KKU-055 and KKU-213A cells. Representative data of (A) CD3 and TNF- α or (B) CD3 and IFN- γ staining in the untransduced (UTD) T, α M.CAR T and α M.CAR/SR T cells with or without exposure to MMNK-1, KKU-055 and KKU-213A cells. The percentages of (C) CD3 $^+$ TNF- α $^+$ or (D) CD3 $^+$ IFN- γ $^+$ cells summarized from four independent experiments (mean \pm standard deviation). (E) Secretion levels of cytokines ($n = 3$) from either UTD T, α M.CAR T or α M.CAR/SR T cells co-cultured with KKU-213A cells. The data were plotted as bar graphs of fold-changes and all datasets were analyzed by the Student *t*-test (* $P < 0.05$, ** $P < 0.01$, *** $P < 0.001$, and **** $P < 0.0001$). (Color version of figure is available online.)

To further evaluate cytokine secretion, the culture supernatants were analyzed by the LEGENDplex cytokine bead array (Fig. 5E). The results showed that levels of TNF- α and IFN- γ secretions were significantly greater after co-culturing of α M.CAR/SR T cells with KKU-213A cells, compared with those of α M.CAR T cells co-cultured with the same target cells ($P = 0.0062$ and 0.0164 , respectively). These results were in accordance with those of the intracellular cytokine study. In addition, compared with UTD T cells, the level of IL-2 secretion was significantly greater after the co-cultures of α M.CAR T cells ($P = 0.0486$) or α M.CAR/SR T cells ($P = 0.0414$) with KKU-213A cells. The IL-2 secretion of α M.CAR/SR T cells was slightly greater than that of the α M.CAR T cells but not statistically significant ($P = 0.427$). Furthermore, there were no significant differences in the levels of immunosuppressive (IL-4 and IL-10) and pro-inflammatory (IL-6) cytokines when α M.CAR T cells or α M.CAR/SR T cells were co-cultured with KKU-213A cells (Fig. 5E).

α M.CAR/SR T cells enhanced anti-tumor cytotoxicity against CCA cells expressing MUC1 and PD-L1

To compare the cytotoxic functions of α M.CAR T cells and α M.CAR/SR T cells against CCA cells, the α M.CAR T or α M.CAR/SR T cells were co-cultured with MMNK-1 cholangiocytes, KKU-055 and KKU-213A cells, which were genetically engineered to stably expressed green fluorescent protein and luciferase enzyme at E:T ratios of 1:1,

2.5:1 and 5:1. The results showed that the UTD T, α M.CAR T and α M.CAR/SR T cells had very low cytotoxic activities against the MMNK-1 cells expressing low MUC1 at all E:T ratios. In contrast, α M.CAR T and α M.CAR/SR T cells obviously induced cytotoxicity against KKU-055 cells and KKU-213A cells expressing high levels of MUC1 (Fig. 6A,B). The reduction of remaining KKU-055 and KKU-213A tumor cells were observed in a dose-dependent manner. At the E:T ratio of 2.5:1, the cytotoxic activities of the UTD T cells against the KKU-055 cells were $11.63 \pm 3.58\%$, whereas those of the α M.CAR T and α M.CAR/SR T cells were $48.59 \pm 21.31\%$ ($P = 0.0141$) and $55.74 \pm 16.17\%$ ($P = 0.0018$), respectively. At the E:T ratio of 5:1, the cytotoxic activities of the UTD T cells against the KKU-055 cells were $32.33 \pm 6.45\%$, whereas those of the α M.CAR T and α M.CAR/SR T cells were $72.66 \pm 12.71\%$ ($P = 0.0013$) and $79.89 \pm 10\%$ ($P = 0.0002$), respectively (Fig. 6B).

In KKU-213A cells, the cytotoxic activities of the α M.CAR T and α M.CAR/SR T cells were significant greater at all E:T ratios, compared with UTD T cells. At the E:T ratio of 1:1, the cytotoxic activities of the α M.CAR T and α M.CAR/SR T cells were $17.1 \pm 5.8\%$ and $27.7 \pm 17\%$, respectively (both $P < 0.05$). The cytotoxic activities of the α M.CAR T and α M.CAR/SR T cells were $27.39 \pm 8.01\%$ ($P = 0.0321$) and $45.11 \pm 16.9\%$ ($P = 0.0114$) at the E:T ratio of 2.5:1, and $47.15 \pm 8.41\%$ ($P = 0.0442$) and $70.69 \pm 14.38\%$ ($P = 0.005$), at the E:T ratio of 5:1, respectively. Importantly, α M.CAR/SR T cells showed significantly higher killing activity than that of α M.CAR T cells against MUC1- and

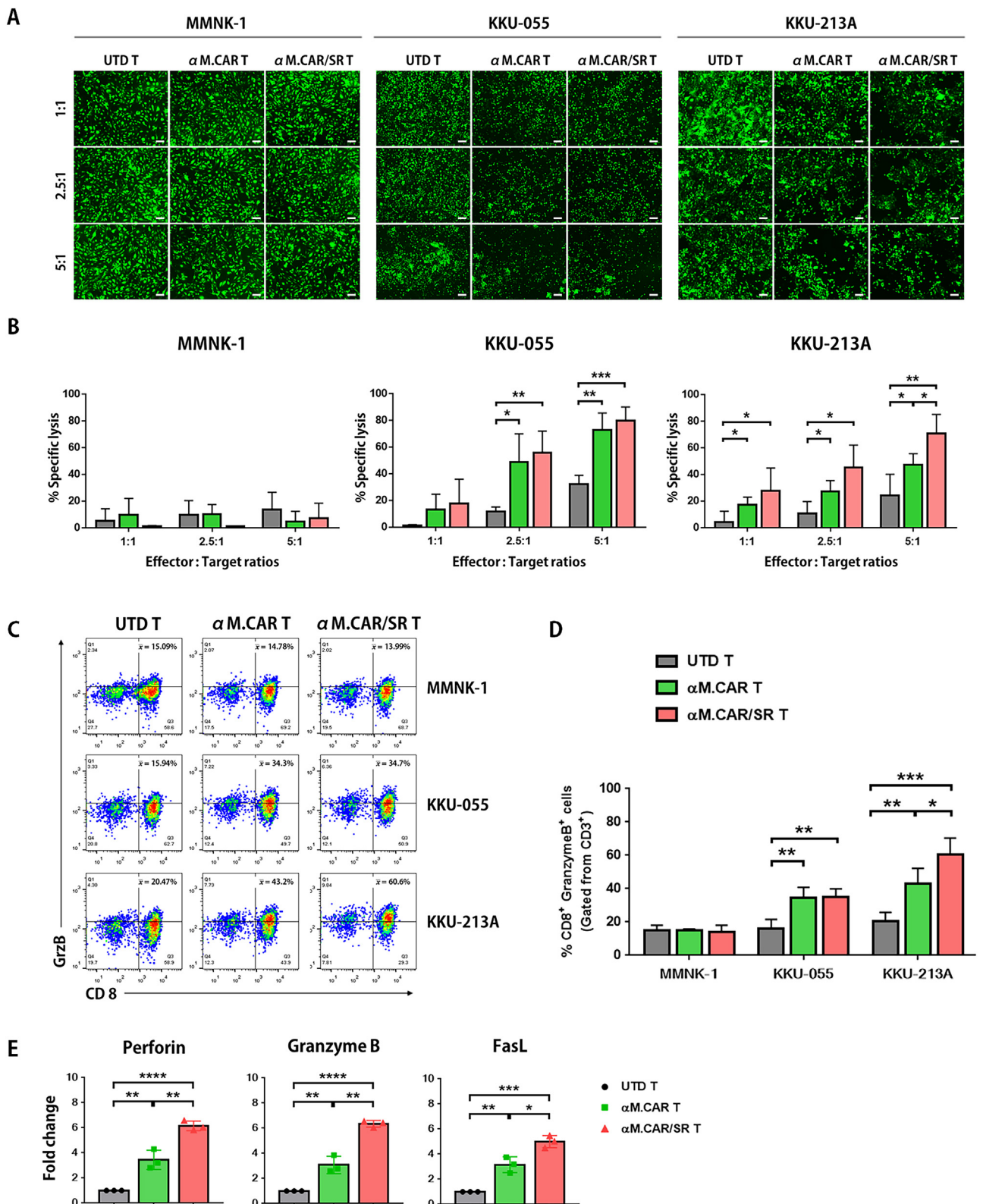


Fig. 6. Cytotoxic functions of α M.CAR T and α M.CAR/SR T cells against cholangiocytes (MMNK-1) and CCA (KKU-055, and KKU-213A) cells, which expressed different levels of MUC1 and PD-L1. (A) Remaining target cells expressing green fluorescence signal captured under a fluorescence microscope after co-culturing with (UTD T cells, α M.CAR T cells and α M.CAR/SR T cells at E:T ratios of 1:1, 2.5:1 and 5:1. The scale bars are 100 μ m. (B) Percentages of specific cell lysis calculated from luciferase activity of remaining target cells after co-culturing with UTD T cells (gray), α M.CAR T cells (green), and α M.CAR/SR T cells (red). (C) Intracellular granzyme B detection in the UTD T cells, α M.CAR T cells and α M.CAR/SR T cells co-cultured with MMNK-1, KKU-055 and KKU-213A cells at an E:T ratio of 5:1. (D) Percentages of CD8⁺ granzyme B⁺ T cells. (E) Secretion levels of effector proteins ($n = 3$) were plotted as bar graphs of fold-changes compared with those of UTD T-cell treatment. All datasets were summarized from three to four independent experiments (mean \pm standard deviation) and statistically analyzed by the Student *t*-test (asterisks indicate: (*) $P < 0.05$, (**) $P < 0.01$, (***) $P < 0.001$, and (****) $P < 0.0001$). (Color version of figure is available online.)

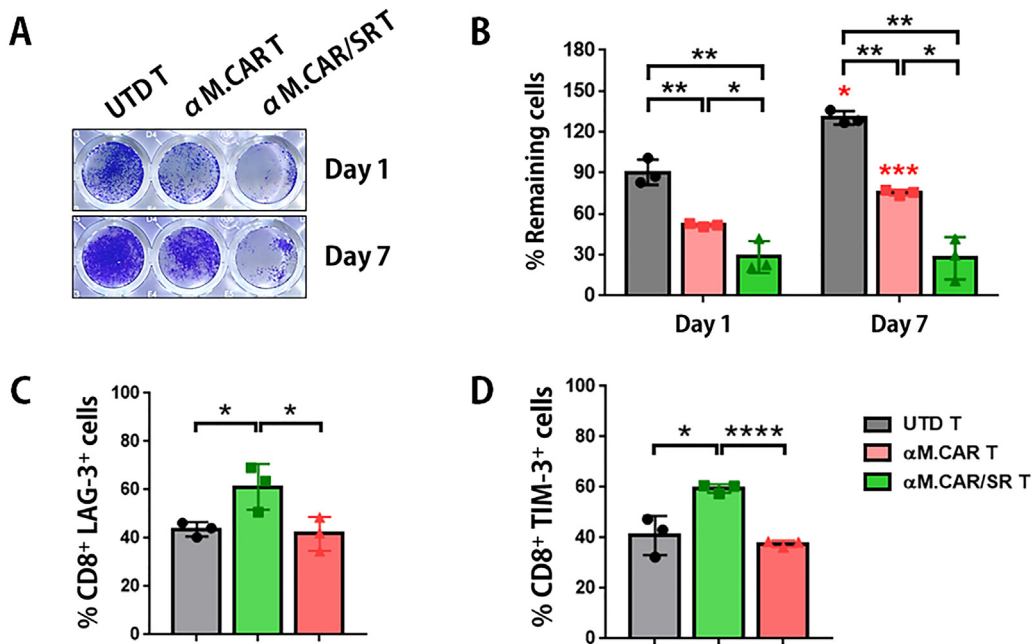


Fig. 7. Cytotoxic function and exhaustion markers of α M.CAR T and α M.CAR/SR T cells after long-term exposure to KKU-213A cells. (A) Representative data of remaining target cells stained with crystal violet after CAR T cell treatments on days 1 and 7. (B) Bar graphs summarized the percentages of remaining target cells from three independent experiments. The black asterisks are the statistical comparisons among the groups of UTD T, α M.CAR T and α M.CAR/SR T cells on day 1 or day 7. The red asterisks are the comparisons of each group on day 1 versus day 7. Evaluation of (C) LAG-3 and (D) TIM-3 expression in UTD T, α M.CAR T and α M.CAR/SR T cells after 7 days of the co-culture (E:T = 2:1) by flow cytometry. Statistical analysis was performed by the Student *t*-test (**P* < 0.05, ***P* < 0.01, ****P* < 0.001, and *****P* < 0.0001). (Color version of figure is available online.)

PD-L1-expressing KKU-213A cells at the E:T ratio of 5:1 (*P* = 0.031). The enhancement of specific KKU-213A cell lysis by addition of SR was approximately 20% (Fig. 6B).

A cytotoxic protein (granzyme B) was examined (Fig. 6C,D). After exposure to the MUC1-expressing tumors, the percentage of CD8⁺ granzyme B⁺ T cells in the α M.CAR T and α M.CAR/SR T cells were significantly greater, compared with UTD T cells. In KKU-055, the percentage of CD8⁺ granzyme B⁺ T cells was 34.3 ± 6.52% in the α M.CAR T (*P* = 0.0051) and 34.77 ± 5.18% in α M.CAR/SR T cells (*P* = 0.0025). Similar fashion was found after exposure to the MUC1- and PD-L1-expressing KKU-213A, the percentage of CD8⁺ granzyme B⁺ T cells in the α M.CAR T and α M.CAR/SR T cells were 43.2 ± 6.52 (*P* = 0.0047) and 60.6 ± 9.89% (*P* = 0.0004), respectively. Importantly, the percentage of CD8⁺ granzyme B⁺ T cells in the α M.CAR/SR T cells was significantly higher than that in the α M.CAR T cells (*P* = 0.0402) (Fig. 6D). It is of note that no significant difference was observed in UTD T, α M.CAR T, and α M.CAR/SR T cells after MMNK-1 exposure.

Secretion levels of effector molecules (perforin, granzyme B and Fas ligand [FasL]) were determined after co-culturing of either α M.CAR T cells or α M.CAR/SR T cells with MUC1⁺PD-L1⁺ cells (KKU-213A) (Fig. 6E). The results showed that significantly greater levels of these effector molecules were observed in the conditions containing α M.CAR T cells (*P* < 0.01) and α M.CAR/SR T cells (*P* < 0.001) compared with UTD T cells. In addition, the levels of these effector molecules were significantly greater after the α M.CAR/SR T-cell treatment compared with those of the α M.CAR T-cell treatment (*P* = 0.0056 for perforin, *P* = 0.0015 for granzyme B and *P* = 0.0158 for FasL).

α M.CAR/SR T cells prolonged cytotoxic function and ameliorated T-cell exhaustion

To investigate α M.CAR/SR T-cell functions after long-term exposure to CCA cells, the CAR T cells were co-cultured with MUC1⁺PD-L1⁺ KKU-213A cells for 7 days. On days 1 and 7, the viable target cells were stained with crystal violet (Fig. 7A). Compared with UTD T cells, the remaining KKU-213A cells were significantly reduced after co-

culturing with α M.CAR T cells or α M.CAR/SR T cells (all *P* < 0.01) (Fig. 7B). The percentages of remaining target cells after co-culturing with α M.CAR/SR T cells (days 1 and 7) were 28.45 ± 11.69%, and 20.46 ± 13.21%, respectively, which were significantly lower than those of α M.CAR T cells, 51.84 ± 1.21%, and 76.76 ± 1.05% (all *P* < 0.05), respectively. Notably, on day 7, the target cancer cells were well controlled by α M.CAR/SR T cells, whereas they recurred after co-culturing with α M.CAR T cells (*P* = 0.0002). Moreover, the levels of exhaustion markers, LAG-3 and TIM-3, were significantly increased in the α M.CAR T cells compared with UTD T cells, *P* = 0.0370 and 0.0154, respectively (Fig. 7C,D). However, their levels were not changed in α M.CAR/SR T cells. These exhaustion markers were significantly reduced in the α M.CAR/SR T cells compared with those of α M.CAR T cells, (*P* = 0.0457 for LAG-3 and *P* < 0.0001 for TIM-3). These results suggested that α M.CAR/SR T cells provided superior anti-tumor activity after long-term co-culture with MUC1⁺PD-L1⁺ CCA cells.

Enhanced cytotoxic function of α M.CAR/SR T cells against KKU213A spheroids

To examine abilities of α M.CAR T cells and α M.CAR/SR T cells in a 3D co-culture system, MUC1- and PD-L1-expressing KKU-213A spheroids were formed and co-cultured with UTD T cells, α M.CAR T cells or α M.CAR/SR T cells at an E:T ratio of 10:1. The spheroids were captured for their destroyed structure and reduced green fluorescence signals under a fluorescence microscope (Fig. 8). Significant disruption of tumor spheroids and reduced green fluorescence signals was found at days 3 and 5 after the CAR T-cell treatment when compared with no-treatment (all *P* < .0001) and UTD T cells (*P* = 0.0098 and *P* < 0.0001 at day 3, and *P* = 0.0014 and *P* = 0.0001 at day 5). Although KKU-213A spheroids were lysed by both α M.CAR T cells and α M.CAR/SR T cells, the latter demonstrated faster and greater extent in tumor destruction. The KKU-213A spheroids were significantly destructed after 24-h co-culture of α M.CAR/SR T cells compared with that of the no-treatment control (*P* = 0.0145). In

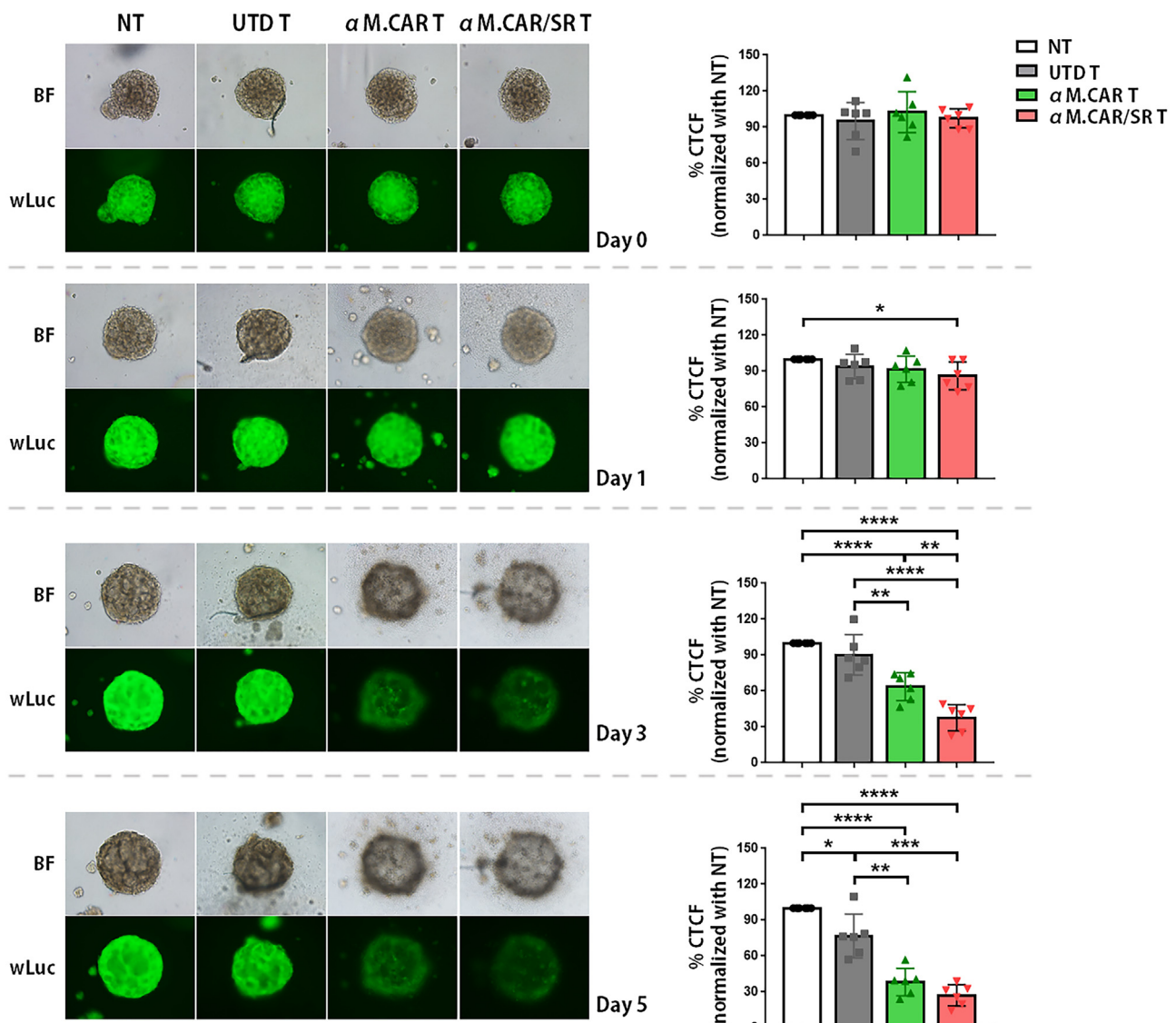


Fig. 8. Cytotoxic functions of α M.CAR T and α M.CAR/SR T cells against MUC1- and PD-L1-expressing KKU-213A spheroids. The representative results of Wasabi-luciferase (wLuc)-expressing KKU-213A spheroids (green fluorescence) cultured with UTD T cells, α M.CAR T cells and α M.CAR/SR T cells (at an E:T ratio of 10:1) are shown. The KKU-213A spheroids with the no-treatment (NT) condition were used as a no-killing control. BF is bright field captured under a fluorescence microscope with the objective lens set at 10 \times magnification. The bar graphs represent the summarized data of CTCF signals obtained from the independent experiments using the cells prepared from six individual donors (mean \pm standard deviation). Statistical analysis was performed by the Student t-test (* P < 0.05, ** P < 0.01, *** P < 0.001, and **** P < 0.0001). (Color version of figure is available online.)

addition, the α M.CAR/SR T cells demonstrated significantly greater disruption of the structure and reduced green fluorescence signals at day 3 after the treatment, compared with that of the treatment with the α M.CAR T cells (P = 0.0027). Overall, our data suggested that the addition of SR in anti-MUC1-CAR T (α M.CAR/SR T cells) could enhance anti-tumor effects.

Discussion

CCA causes very high mortality rates worldwide without efficient curative approaches in the advanced stage of the disease [1]. Novel therapeutic approaches with high efficacy are urgently required. MUC1 expression is associated with poor prognosis in patients with CCA [6–9]. Also, MUC1 overexpression is reported to be related with PD-L1 upregulation in solid cancers [12–14]. Nevertheless, data regarding the association between MUC1 and PD-L1 expression in different subtypes of CCA are limited. The MUC1 expression was reported in extrahepatic CCA (72.5%) and intrahepatic CCA (iCCA;

55.8%) subtypes [1], and also in *Opisthorchis viverrini* (OV)-related iCCA (77%) [2]. Although PD-L1 expression predominated in iCCA (71.7%) [3], it was found in another report that iCCA (19.7%) and perihilar CCA (36.6%) with dense intratumoral inflammatory cells were positive for PD-L1 expression [4]. MUC1-mediated PD-L1 expression may inhibit CAR T-cell functions via the PD-1/PD-L1 pathway. Thus, in the present study, anti-MUC1 CAR T cells with the addition of PD-1-CD28 SR (α M.CAR/SR T cells) were developed to target CCA cells to enhance tumor cytotoxic function in the presence of PD-L1 inhibitory ligands in CCA. We also initially tested whether alteration of MUC1 could have an effect on PD-L1 expression, and our results suggested that greater expression levels of MUC1 may contribute to greater PD-L1 levels in this particular CCA models (Fig. 1 and supplementary Fig. 1C). The possible mechanisms of MUC1-mediated PD-L1 upregulation could be occurred via (i) activation of nuclear factor kappa-light-chain-enhancer of activated B cells (NF- κ B) pathway and (ii) induction of MYC protein. The upstream of transcriptional start site of the PD-L1 gene contains an NF- κ B p65-binding site and also an

MYC binding site (E-box sequence) [12–14]. However, the underlying mechanism of how MUC1 regulates PD-L1 in CCA cells should be further investigated.

To simultaneously target MUC-1– and PD-L1–expressing CCA cells, we generated α M.CAR/SR T cells using a lentiviral system. The major populations of cytotoxic CD8⁺ T cells and effector memory T cells in the α M.CAR/SR T cells (Fig. 4A,F) could be promoted by PHA activation [35], cytokines (IL-2, IL-7 and IL-15) added in the culture media [36,37] and probably also the co-stimulatory molecule (CD137) generated from the CAR construct [38]. Since the cytotoxic (CD8⁺) T cells are the major population mediating antigen-specific target cell lysis [39], their increase may benefit the clearance of cancer cells. Effector memory (CD45RA⁻ CD62L⁻) T cells are cells containing high cytotoxic and persistent capabilities, which prefer to locate in inflamed tissues to control infected and cancerous cells [40]. Although the levels of activation markers between α M.CAR T cells and α M.CAR/SR T cells were not different, the latter showed significantly lower proportions of the exhaustion (LAG-3 and TIM-3) markers, which were detected at the baseline levels (Fig. 4C–E). The attenuated T-cell exhaustion might be due to the parallel expressions of CD28 from the SR and CD137 from the CAR molecule [41]. LAG-3 and TIM-3 are the immune checkpoint molecules essential for maintaining immune cell homeostasis and regulating T-cell function. LAG-3 is normally expressed on the activated CD4⁺ T, CD8⁺ T, regulatory T and NK cells whereas TIM-3 is found on the CD4⁺ T, CD8⁺ T, regulatory T and innate immune cells. When these proteins bind to their ligands, cell proliferation and cytokine production of T cells are inhibited but regulatory T functions are promoted [42]. The exact mechanisms of how the presence of SR could diminish the exhaustion marker expressions should be further investigated.

In this particular model, the comparison of α M.CAR T cells and α M.CAR/SR T cells demonstrated enhanced T-cell proliferation, cytokine productions and anti-tumor effects by the addition of PD-1-CD28 SR. The specific expansion of the α M.CAR/SR T cells was shown only when they were exposed to MUC1⁺PD-L1⁺ CCA cells but not MMNK-1 cholangiocytes, suggesting that the expansion of α M.CAR/SR T cells was specific to the expression of MUC1 and PD-L1 (Fig. 3D). Moreover, the expansion of the α M.CAR/SR T cells was greater than that of the α M.CAR T cells, inferring to the ability of the SR molecules in enhancing the expansion of α M.CAR/SR T cells through the PD-L1/PD1 interaction. Our results were in accordance with previous studies in other solid-tumor models [30,31].

TNF- α is secreted from T and innate immune cells to promote cell proliferation, differentiation and inflammatory responses. Moreover, it also contributes to target cell death, depending on the signal transduction [43]. IFN- γ is mainly produced from T, NK and NKT cells in response to pathogen infection and cancers [44]. Intracellular cytokine (TNF- α and IFN- γ) production was induced by CCA expressing MUC1 in an antigen-dependent manner, whereas it was not induced by cholangiocytes (MMNK-1 cells) expressing low MUC1. Our data are correlated with previous finding that the expression of SR could enhance intracellular TNF- α and IFN- γ cytokine productions (Fig. 5) [30–32]. The cytotoxic activity of the α M.CAR/SR T cells was found the greatest up to 80% after the co-culturing with CCA cells expressing MUC1 and PD-L1, compared with those of the UTD T cells and α M.CAR T cells (Fig. 6A,B). Concurrently, the α M.CAR/SR T cells showed increased perforin, granzyme B and FasL upon exposure to CCA-expressing MUC1 and PD-L1 (Fig. 6C–E). Perforin is a pore-forming cytolytic protein and granzyme B is a cytotoxic protease contained in granules within the T cells. After the receptor binding and T-cell activation, perforin and granzyme B were released from the cytotoxic granules. Perforin provides the pore formation that allows granzyme B to penetrate target cells and induce cellular apoptosis [45]. FasL mediates target cell apoptosis via binding to its receptor and activating caspase cascade pathway [46]. Overall data suggest

the enhance anti-tumor effects by the addition of PD1-CD28 SR in the α M.CAR/SR T cells.

It is noteworthy that the cytotoxic activities of the α M.CAR T cells and α M.CAR/SR T cells against the KKU-055 cells at the E:T ratio of 5:1 were not different and high as $72.66 \pm 12.71\%$ and $79.89 \pm 10\%$, respectively, whereas the anti-tumor effect of α M.CAR T cells ($47.15 \pm 8.41\%$) was much lower compared with the α M.CAR/SR T cells ($70.69 \pm 14.38\%$) in high PD-L1 expressing KKU-213A cells (Fig. 6). Our results suggested that tumor cells with low PD-L1 expression were susceptible to be killed by α M.CAR T cells partly due to low expression of PD-L1 in the KKU-055 cells; however, high PD-L1 expression on KKU-213A cells could inhibit α M.CAR T cell function, which could be overcome by addition of PD-1-CD28 SR to the CAR T cells. Furthermore, the α M.CAR/SR T cells exhibited significant killing efficacy in long-term (7 days) of co-culturing with KKU-213A cells, in addition to lower levels of exhaustion markers (Fig. 7), suggesting that the α M.CAR/SR T cells were less susceptible to tumor resistance. Although endogenous PD-1 expression on T cells could be upregulated upon TCR activation when they were exposed to target antigens [47] or prolong cytokine treatments, our results demonstrated that α M.CAR/SR T cells were still effective in killing MUC1⁺PD-L1⁺ KKU-213A cells, as illustrated by increased T-cell proliferation, cytotoxic function and cytokine secretion (Fig. 3D, 5, and 6). Thus, it is possible that, in the presence of endogenous PD-1, inducible PD-1 in the α M.CAR/SR T cells was able to switch the inhibitory to activating signal to enhance CAR T-cell function. Our results are in accordance to a previous study that endogenous PD-1 expression did not interfere with the function of CAR T cells expressing SR [30].

In addition, we also demonstrated the significant enhancement of cytotoxic function of the α M.CAR/SR T cells against KKU-213A cells cultured as a 3D spheroid (Fig. 8). The 3D-cultured spheroid represents a model closer to solid tumor *in vivo* than the two-dimensional-cultured model [48]. Our results showed that the KKU-213A spheroids were significantly destroyed by α M.CAR/SR T cells on day 3 when compared with that by α M.CAR T cells. The overall results suggested the potential of α M.CAR/SR T cells for use as an alternative treatment of MUC1- and PD-L1-expressing CCA. Still, the efficacy of α M.CAR/SR T cells needs to be further investigated *in vivo* in several aspects, including CAR T-cell penetration, proliferation and persistence, reduction of tumor growth, prolonged animal survival and safety. These effects should be validated in one or more animal models to rule out any possible influence caused by the inherent inconsistency between *in vitro* and *in vivo* conditions.

Although the impressive efficiencies of the α M.CAR/SR T cells against CCA cells expressing MUC1 and PD-L1 were demonstrated, some limitations exist in the present study. First, all of the CCA cell lines used in this study had the etiology associated with chronic liver fluke infection. Other CCA cell lines related to different predisposing factors such as primary sclerosing cholangitis should be further investigated. However, previous studies reported that MUC1 expression was approximately 50–86.5% in both OV- and non-OV-related CCA patient tissues [6–8], and also 56% in primary sclerosing cholangitis–related CCA [49]. Thus, our α M.CAR/SR T cells would provide a possible option for those populations of patients with CCA with MUC1⁺ phenotype. Assessment of MUC1 expression is required before the application of this CAR T-cell immunotherapy. Second, the PD-L1 overexpression in CCA is not only one challenge for cancer immunotherapy. Other tumor microenvironments of CCA, including tumor-associated macrophages, cancer-associated fibroblasts, immunosuppressive cytokines (IL-10 and TGF- β) and other immune checkpoint molecules (CTLA-4, LAG-3 and TIM-3) should also be concerned [50]. Third, since the α M.CAR/SR T cells were modified to be resisted to immune checkpoint regulation, these may cause adverse side effects and uncontrollable responses. Hence, adding suicide genes, including inducible-caspase-9 and herpes simplex–thymidine kinase

[51], may be further studied to eliminate the CAR T cells if it is necessary.

In summary, our results suggest that MUC1 modulates PD-L1 expression in CCA cells. α M.CAR/SR T cells were successfully generated and evaluated against CCA cells expressing MUC1 and PD-L1. The populations of α M.CAR/SR T cells were mainly cytotoxic T cells with increased memory and decreased exhaustion phenotypes. The overall results support the markedly enhanced cytotoxicity of α M.CAR/SR T cells against CCA cells expressing MUC1 and PD-L1, as demonstrated by (i) the enhancement of T-cell proliferation, (ii) the greater cytokine production, (iii) the increased killing activity in the two-dimensional co-culture system, (iv) the greater granzyme B production and (v) the enhanced destruction of the co-cultured 3D-spheroids. These results provide the evidence of using α M.CAR/SR T cells to overcome inhibitory signals of the immune checkpoint molecule, PD-L1, in CCA cells, which should be further developed for CCA treatment.

Declaration of Competing Interest

The authors have no commercial, proprietary, or financial interest in the products or companies described in this article.

Funding

This work was supported by the Siriraj Research Fund, Faculty of Medicine Siriraj Hospital, Mahidol University (grant nos. R016034008 and R016334002), Mahidol University (grant nos. R015810005 and R016110006), and International Research Network (IRN) (IRN58W0001), Thailand Research Fund (TRF). KS and TS were formerly supported by IRN Scholarships (IRN5801PHDW04 and IRN5801PHDW02) and Siriraj Graduate Scholarships, Faculty of Medicine Siriraj Hospital, Mahidol University. MJ was supported by Siriraj Chalermphrakiat Grant.

Author Contributions

Conception and design of the study: all authors. Acquisition of data: KS and TS. Analysis and interpretation of data: KS and PY. Drafting or revising the manuscript: KS, TS, MJ, and PY. All authors have approved the final article.

Acknowledgments

We thank Dr. John Maher for the provision of materials.

Supplementary materials

Supplementary material associated with this article can be found in the online version at doi:[10.1016/j.jcyt.2022.10.006](https://doi.org/10.1016/j.jcyt.2022.10.006).

References

- [1] Banales JM, Marin JJJG, Lamarca A, Rodrigues PM, Khan SA, Roberts LR, et al. Cholangiocarcinoma 2020: the next horizon in mechanisms and management. *Nat Rev Gastroenterol Hepatol* 2020;17(9):557–88.
- [2] Blehacz BR, Gores GJ. Cholangiocarcinoma. *Clin Liver Dis* 2008;12(1):131–50. ix.
- [3] Andre T, Reyes-Vidal JM, Fartoux L, Ross P, Leslie M, Rosmorduc O, et al. Gemcitabine and oxaliplatin in advanced biliary tract carcinoma: a phase II study. *Br J Cancer* 2008;99(6):862–7.
- [4] Chai Y. Immunotherapy of biliary tract cancer. *Tumour Biol* 2016;37(3):2817–21.
- [5] Loeillard E, Conboy CB, Gores GJ, Rizvi S. Immunobiology of cholangiocarcinoma. *JHEP reports : innovation in hepatology* 2019;1(4):297–311.
- [6] Boonla C, Srija B, Thuwajit P, Cha-On U, Puapairoj A, Miwa M, et al. MUC1 and MUC5AC mucin expression in liver fluke-associated intrahepatic cholangiocarcinoma. *World J Gastroenterol* 2005;11(32):4939–46.
- [7] Yuan SF, Li KZ, Wang L, Dou KF, Yan Z, Han W, et al. Expression of MUC1 and its significance in hepatocellular and cholangiocarcinoma tissue. *World J Gastroenterol* 2005;11(30):4661–6.
- [8] Park SY, Roh SJ, Kim YN, Kim SZ, Park HS, Jang KY, et al. Expression of MUC1, MUC2, MUC5AC and MUC6 in cholangiocarcinoma: prognostic impact. *Oncol Rep* 2009;22(3):649–57.
- [9] Horm TM, Schroeder JA. MUC1 and metastatic cancer: expression, function and therapeutic targeting. *Cell adhesion & migration* 2013;7(2):187–98.
- [10] Nath S, Mukherjee P. MUC1: a multifaceted oncoprotein with a key role in cancer progression. *Trends Mol Med* 2014;20(6):332–42.
- [11] Dhar P, McAuley J. The role of the cell surface mucin MUC1 as a barrier to infection and regulator of inflammation. 2019;9(117).
- [12] Bouillez A, Rajabi H, Jin C, Samur M, Tagde A, Alam M, et al. MUC1-C integrates PD-L1 induction with repression of immune effectors in non-small-cell lung cancer. *Oncogene* 2017;36(28):4037–46.
- [13] Pyzer AR, Stroopinsky D, Rosenblatt J, Anastasiadou E, Rajabi H, Washington A, et al. MUC1 inhibition leads to decrease in PD-L1 levels via upregulation of miRNAs. *Leukemia* 2017;31(12):2780–90.
- [14] Maeda T, Hiraki M, Jin C, Rajabi H, Tagde A, Alam M, et al. MUC1-C Induces PD-L1 and Immune Evasion in Triple-Negative Breast Cancer. *Cancer Res* 2018;78(1):205–15.
- [15] Han Y, Liu D, Li L. PD-1/PD-L1 pathway: current researches in cancer. *Am J Cancer Res* 2020;10(3):727–42.
- [16] Sharpe AH, Pauken KE. The diverse functions of the PD1 inhibitory pathway. *Nat Rev Immunol* 2018;18(3):153–67.
- [17] Chabanon RM, Pedrero M, Lefebvre C, Marabelle A, Soria JC, Postel-Vinay S. Mutational landscape and sensitivity to immune checkpoint blockers. *Clin Cancer Res* 2016;22(17):4309–21.
- [18] Sangkhamanon S, Jongpairoat P, Sookprasert A, Wirasorn K, Titapun A, Pugkhem A, et al. Programmed death-ligand 1 (PD-L1) expression associated with a high neutrophil/lymphocyte ratio in cholangiocarcinoma. *Asian Pac J Cancer Prev* 2017;18(6):1671–4.
- [19] Ahn S, Lee JC, Shin DW, Kim J, Hwang JH. High PD-L1 expression is associated with therapeutic response to pembrolizumab in patients with advanced biliary tract cancer. *Sci Rep* 2020;10(1):12348.
- [20] Ma S, Li X, Wang X, Cheng L, Li Z, Zhang C, et al. Current progress in CAR-T cell therapy for solid tumors. *Int J Biol Sci* 2019;15(12):2548–60.
- [21] Maude SL, Laetsch TW, Buechner J, Rives S, Boyer M, Bittencourt H, et al. Tisagenlecleucel in children and young adults with B-cell lymphoblastic leukemia. *N Engl J Med* 2018;378(5):439–48.
- [22] Wilkie S, Picco G, Foster J, Davies DM, Julien S, Cooper L, et al. Retargeting of human T cells to tumor-associated MUC1: the evolution of a chimeric antigen receptor. *J Immunol* 2008;180(7):4901–9.
- [23] Posey Jr. AD, Schwab RD, Boesteanu AC, Steentoft C, Mandel U, Engels B, et al. Engineered CAR T cells targeting the cancer-associated Tn-glycoform of the membrane mucin MUC1 control adenocarcinoma. *Immunity* 2016;44(6):1444–54.
- [24] Bajgain P, Tawinwung S, D'Elia L, Sukumaran S, Watanabe N, Hoyos V, et al. CAR T cell therapy for breast cancer: harnessing the tumor milieu to drive T cell activation. *J Immunother Cancer* 2018;6(1):34.
- [25] Zhou R, Yazdanifar M, Roy LD, Wildling LM, Gavril A, Maher J, et al. CAR T cells targeting the tumor MUC1 glycoprotein reduce triple-negative breast cancer growth. *Front Immunol* 2019;10:1149.
- [26] Mei Z, Zhang K, Lam AK, Huang J, Qiu F, Qiao B, et al. MUC1 as a target for CAR-T therapy in head and neck squamous cell carcinoma. *Cancer medicine* 2020;9(2):640–52.
- [27] Supimon K, Sangsuwanukul T, Sujitjoon J, Phanthaphol N, Chieochansin T, Poungvarin N, et al. Anti-mucin 1 chimeric antigen receptor T cells for adoptive T cell therapy of cholangiocarcinoma. *Sci Rep* 2021;11(1):6276.
- [28] Taylor-Papadimitriou J, Burchell JM, Graham R, Beatson R. Latest developments in MUC1 immunotherapy. *Biochem Soc Trans* 2018;46(3):659–68.
- [29] Yeku OO, Purdon TJ, Koneru M, Spriggs D, Brentjens RJ. Armored CAR T cells enhance antitumor efficacy and overcome the tumor microenvironment. *Sci Rep* 2017;7(1):10541.
- [30] Liu X, Ranganathan R, Jiang S, Fang C, Sun J, Kim S, et al. A chimeric switch-receptor targeting PD1 augments the efficacy of second-generation CAR T cells in advanced solid tumors. *Cancer Res* 2016;76(6):1578–90.
- [31] Huang B, Luo L, Wang J, He B, Feng R, Xian N, et al. B7-H3 specific T cells with chimeric antigen receptor and decoy PD-1 receptors eradicate established solid human tumors in mouse models. *Oncimmunology* 2020;9(1):1684127.
- [32] Chen C, Gu YM, Zhang F, Zhang ZC, Zhang YT, He YD, et al. Construction of PD1/CD28 chimeric-switch receptor enhances anti-tumor ability of c-Met CAR-T in gastric cancer. *Oncimmunology* 2021;10(1):1901434.
- [33] Schneider CA, Rasband WS, Eliceiri KW. NIH Image to ImageJ: 25 years of image analysis. *Nature methods* 2012;9(7):671–5.
- [34] Martinez M, Moon EK. CAR T cells for solid tumors: new strategies for finding, infiltrating, and surviving in the tumor microenvironment. *Front Immunol* 2019;10:128.
- [35] Lomakova YD, Londregan J, Maslanka J, Goldman N, Somerville J, Riggs JE. PHA eludes macrophage suppression to activate CD8(+) T cells. *Immunobiology* 2019;224(1):94–101.

- [36] Montes M, Rufer N, Appay V, Reynard S, Pittet MJ, Speiser DE, et al. Optimum in vitro expansion of human antigen-specific CD8 T cells for adoptive transfer therapy. *Clin Exp Immunol* 2005;142(2):292–302.
- [37] McLellan AD, Ali-Hosseini-Rad SM. Chimeric antigen receptor T cell persistence and memory cell formation. *Immunol Cell Biol* 2019;97(7):664–74.
- [38] Zhang H, Snyder KM, Suhoski MM, Maus MV, Kapoor V, June CH, et al. 4-1BB is superior to CD28 costimulation for generating CD8+ cytotoxic lymphocytes for adoptive immunotherapy. *J Immunol* 2007;179(7):4910–8.
- [39] Zhang N, Bevan MJ. CD8(+) T cells: foot soldiers of the immune system. *Immunity* 2011;35(2):161–8.
- [40] Martin MD, Badovinac VP. Defining memory CD8 T cell. *Front Immunol*. 2018;9:2692.
- [41] Muliaditan T, Halim L, Whilding LM, Draper B, Achkova DY, Kausar F, et al. Synergistic T cell signaling by 41BB and CD28 is optimally achieved by membrane proximal positioning within parallel chimeric antigen receptors. *Cell Reports Medicine* 2021;2(12):100457.
- [42] Anderson AC, Joller N, Kuchroo VK. Lag-3, Tim-3, and TIGIT: Co-inhibitory receptors with specialized functions in immune regulation. *Immunity* 2016;44(5):989–1004.
- [43] Brenner D, Blaser H, Mak TW. Regulation of tumour necrosis factor signalling: live or let die. *Nat Rev Immunol* 2015;15(6):362–74.
- [44] Ni L, Lu J. Interferon gamma in cancer immunotherapy. *Cancer Med* 2018;7(9):4509–16.
- [45] Cullen SP, Brunet M, Martin SJ. Granzymes in cancer and immunity. *Cell Death Differ* 2010;17(4):616–23.
- [46] Volpe E, Sambucci M, Battistini L, Borsig G. Fas-Fas ligand: checkpoint of T cell functions in multiple sclerosis. *Front Immunol* 2016;7:382.
- [47] Simon S, Labarriere N. PD-1 expression on tumor-specific T cells: Friend or foe for immunotherapy? *Oncimmunology* 2017;7(1):e1364828.
- [48] Katt ME, Placone AL, Wong AD, Xu ZS, Seerson PC. In vitro tumor models: Advantages, disadvantages, variables, and selecting the right platform. *Front Bioeng Biotechnol* 2016;4:12.
- [49] Zen Y, Quaglia A, Heaton N, Rela M, Portmann B. Two distinct pathways of carcinogenesis in primary sclerosing cholangitis. *Histopathology* 2011;59(6):1100–10.
- [50] Fabris L, Sato K, Alpini G, Strazzabosco M. The tumor microenvironment in cholangiocarcinoma progression. *Hepatology* 2021;73(1):75–85. Suppl.
- [51] Yu S, Yi M, Qin S, Wu K. Next generation chimeric antigen receptor T cells: safety strategies to overcome toxicity. *Mol Cancer* 2019;18(1):125.